Int. J. Solids Structures, 1969, Vol. 5, pp. 1259 to 1274. Pergamon Press. Printed in Great Britain.

NUMERICAL SOLUTIONS IN THREE DIMENSIONAL ELASTOSTATICS

T. A. CRUSE

Carnegie-Mellon University, Pittsburgh, Pennsylvania

Abstract—A numerical solution capability is developed for the solution of problems in three dimensional elastostatics. The solution method utilizes singular integral equations which can be solved numerically for the unknown surface tractions and displacements for the fully mixed boundary value problem. The method is independent of the surface shape and data specification and has been fully automated. Some sample problems are solved to verify the formulation. In addition the method has been used to investigate a significant problem with stress singularities.

INTRODUCTION

THE considerable success achieved using integral equations in the analysis of two dimensional elastostatics [1], transient elastodynamics [2, 3], and elastic inclusions [4] leads one to consider extending the solution capability to three-dimensional problems. The solution method utilizes the numerical solution of integral equations analogous to Green's boundary formula in potential theory. It is referred to in this paper as the direct potential method. In the direct potential method integral equations are written directly in terms of the physical boundary tractions and displacements with no need to introduce non-physical potentials or other auxiliary functions. The advantages to the analyst using the direct potential method are the reduced dimension of the numerical problem (the approximations and numerical analysis take place only at the surface) and its great generality. The method employs only real, physical variables and is independent of body shape and connectivity. Most importantly, the method appears to be a valuable new tool in the analysis of three-dimensional problems. The present analysis considers the extension of the direct potential method to problems of three dimensional elastostatics.

The direct potential method is restricted to linear elasticity but may be applied with equal ease for any boundary configuration to the displacement problem, the traction problem and to the fully mixed boundary value problem. The method contrasts with solution methods in three dimensional elasticity based on special geometries and the use of transforms such as in [5]. The method also contrasts with numerical procedures such as finite elements [6] and finite differences [7] in that numerical approximations are made only for the surface tractions and displacements and not on the entire field.

The numerical solution of the integral equations shows remarkable stability as to the surface element arrangements thus allowing efficient analysis of problems with stress concentrations. One such problem, the axial tension member with a completely fixed end, is investigated numerically in this paper and the results compared to available data in the two dimensional counterpart. The numerical procedures have been completely automated and the results obtained on the UNIVAC 1108 computer. Three dimensional problems with cracks and internal voids are now being investigated.

The notation used in this paper is the usual Cartesian tensor notation with implied summation on repeated indices and partial differentiation denoted by the comma-index. The integral equations and the vector and tensor identities for the interior displacements and stresses are derived in the first part of this paper. The numerical solution of the integral equations is discussed in part two and in the third part the method is applied to some example problems.

INTEGRAL EQUATION FORMULATION

The analysis in this paper is restricted to the analysis of classical elastostatic problems for which the material may be taken as isotropic and homogeneous. The usual Navier equations of equilibrium in the absence of body forces and for Poisson's ratio ν are given by

$$\frac{1}{1-2\nu}u_{i,ij}+u_{j,ii} = 0 \qquad (i,j = 1,2,3) \tag{1}$$

for the displacement vector, $u_i(x)$ where x denotes the orthogonal cartesian coordinates x_1, x_2, x_3. The solution to this differential equation must also satisfy appropriate boundary conditions for the displacements and tractions on the surface S, respectively given as

$$u_i(x) = q_i, \qquad x \in S_{(u_i)}$$

and (2)

$$t_i(x) = \sigma_{ij}n_j = p_i, \qquad x \in S_{(t_i)}.$$

The unit vector n_i is the *outward* normal vector for the body R. The stress components σ_{ij} and displacement gradients are related by Hooke's law

$$\sigma_{ij} = \frac{2\mu\nu}{1-2\nu}\delta_{ij}u_{m,m}+\mu(u_{i,j}+u_{j,i}) \tag{3}$$

where μ is the shear modulus of the material.

Letting the distance between the field point x with coordinates x_1, x_2 and x_3 and the load point p with coordinates ξ_1, ξ_2 and ξ_3 be given by

$$r = [(x_i-\xi_i)(x_i-\xi_i)]^{\frac{1}{2}} \tag{4}$$

the well known solution [8] to Kelvin's problem of the point load in the infinite body is represented by the tensor field

$$U_{ij} = \frac{1}{4\pi\mu}\left(\frac{1}{r}\right)\left[\frac{3-4\nu}{4(1-\nu)}\delta_{ij}+\frac{1}{4(1-\nu)}r_{,i}r_{,j}\right]. \tag{5}$$

The displacement and traction vectors corresponding to point loads in each of the three coordinate directions are given by the operations

$$u_j = U_{ij}e_i, \qquad t_j = T_{ij}e_i \tag{6}$$

on the base vectors e_i. In equation (5) and in what follows all differentiation is with respect to the field point x, that is

$$r_{,i} = \frac{\partial r}{\partial x_i} = \frac{1}{r}(x_i-\xi_i)$$

and

$$\frac{\partial r}{\partial n} = \frac{\partial r}{\partial x_i} n_i = \frac{1}{r}(x_i - \xi_i) n_i$$

where the normal is evaluated at x also. The traction vectors for Kelvin's problem are determined from equation (5) and are given by the tensor components,

$$T_{ij} = -\frac{k}{4\pi}\left(\frac{1}{r^2}\right)\left[\frac{\partial r}{\partial n}\left(\delta_{ij} + \frac{3}{1-2v} r_{,i} r_{,j}\right) - n_j r_{,i} + n_i r_{,j}\right], \tag{7}$$

where $k = [(1-2v)/2(1-v)]$.

Now letting the load point p be surrounded by a small spherical region, R^*, with the surface, S^*, Betti's third identity may be written as

$$\int_{S+S^*} (u_i T_{ji} - t_i U_{ji})\, \mathrm{d}S = 0, \tag{8}$$

where u_i, t_i are the displacements and tractions for the unknown stress state. By taking the limits for $R^* \to 0$ in the usual way (see [2]) the following identity results

$$u_j(p) = -\int_S u_i(Q) T_{ji}(Q, p)\, \mathrm{d}S(Q) + \int_S t_i(Q) U_{ji}(Q, p)\, \mathrm{d}S(Q), \tag{9}$$

for the boundary point $Q(x)$. Equation (9) is Somigliana's identity for the displacements [8, p. 245] inside the body, R, due to known surface tractions and displacements. The interior stress state may be generated by differentiation of equation (9) with respect to the load point p and is given by

$$\sigma_{ij}(p) = -\int_S u_k(Q) S_{kij}(Q, p)\, \mathrm{d}S(Q) + \int_S t_k(Q) D_{kij}(Q, p)\, \mathrm{d}S(Q). \tag{10}$$

By utilizing the identity

$$\frac{\partial r}{\partial x_i} = -\frac{\partial r}{\partial \xi_i} \tag{11}$$

the tensors D_{kij} and S_{kij} are found to be

$$D_{kij} = \frac{k}{4\pi}\left(\frac{1}{r^2}\right)\left(\delta_{ki} r_{,j} + \delta_{kj} r_{,i} - \delta_{ij} r_{,k} + \frac{3}{1-2v} r_{,i} r_{,j} r_{,k}\right) \tag{12}$$

and

$$S_{kij} = \frac{k\mu}{4\pi}\left(\frac{2}{r^3}\right)\left\{3\frac{\partial r}{\partial n}\left[\delta_{ij} r_{,k} + \frac{v}{1-2v}(\delta_{ki} r_{,j} + \delta_{kj} r_{,i}) - \frac{5}{1-2v} r_{,i} r_{,j} r_{,k}\right]\right.$$
$$\left. + \frac{3v}{1-2v}(n_i r_{,j} r_{,k} + n_j r_{,i} r_{,k}) + 3n_k r_{,i} r_{,j} + n_j \delta_{ki} + n_i \delta_{kj} - \frac{1-4v}{1-2v} n_k \delta_{ij}\right\}. \tag{13}$$

A number of schemes have been proposed for the solution of equation (9). The Russian mechanicians [9–11] have determined similar equations for the two and three dimensional elasticity problems. The method they have proposed for the solution of equation (9) involves the introduction of auxiliary functions or surface densities which replace the unknown surface tractions and displacements. Using standard procedures of potential theory [12] they obtain approximate relations for the surface density functions. However, recent work [13] has shown that this procedure does not apply for surfaces which are not smooth in the sense of Liapounov.

Another procedure for the solution of equations of the type similar to equation (9) was recently developed [1] for two dimensional elastostatic problems and extended [2, 3] to the two dimensional elastodynamic problems. This paper reports the successful extension of this work to the three dimensional elastostatic problem. It is found that the method suffers none of the numerical instabilities indicated in [13].

Let $P(x)$ be a boundary point distinct from $Q(x)$. If the interior point $p(x)$ in equation (9) is taken to approach point P from within the body a limiting form of equation (9) is obtained. A discussion of this procedure is contained in Appendix 1. The limiting form of equation (9) which is valid for $P(x)$ not located at an edge or corner is given by

$$\frac{1}{2}u_j(P)+\int_S u_i(Q)T_{ji}(Q,P)\,\mathrm{d}S(Q)=\int_S t_i(Q)U_{ji}(Q,P)\,\mathrm{d}S(Q) \tag{14}$$

where the integrals are interpreted in the sense of the Cauchy Principal Value.

Equation (14) can be viewed as the constraint equation relating surface tractions to surface displacements. In physical problems the tractions and displacements are not known concurrently over the entire surface. Thus, the mechanism of solution is to regard equation (14) as a set of coupled integral equations of varying types according as data appropriate to the traction, displacement or mixed boundary value problems are prescribed. The unknowns of the integral equations are the remaining data not prescribed. The numerical solution of equation (14) is discussed in the following section.

NUMERICAL SOLUTION OF THE INTEGRAL EQUATIONS

General analytic solutions to the integral equations (14) are not available and it is therefore necessary to solve the equations numerically. The integral equations reduce to algebraic equations by discretizing the boundary data. Following the procedure used previously in acoustics [14] the two-dimensional surface, S, is assumed to be made up of plane triangular elements, ΔS_i. Although attempts have been made [15] to account for the surface curvature this can only be done approximately and imposes a large burden on the analysis. As important simplifications in the analysis occur by assuming plane surface elements and since many physical problems involve flat surfaces the assumption is made that the surface is piecewise flat. It is further assumed that on each element ΔS_i of the surface the surface data of traction and displacement may be assumed constant. Each surface element is denoted by its centroidal point, Pm or Qn, depending on whether the point is fixed or variable with respect to the integration.

When the surface data is discretized in this way, the integral equations (14) may be seen to reduce to the following algebraic equations.

$$\frac{1}{2}u_j(Pm)+\sum_n u_i(Qn)\int_{\Delta S_n} T_{ji}(Pm,Q)\,\mathrm{d}S(Q)=\sum_n t_i(Qn)\int_{\Delta S_n} U_{ji}(Pm,Q)\,\mathrm{d}S(Q). \tag{15}$$

The values $u_i(Qn)$, $t_i(Qn)$ are now the constant approximations to u_i, t_i on element ΔS_n. The integrals

$$\Delta T_{ij}(Pm, Qn) = \int_{\Delta S_n} T_{ij}(Pm, Q)\, \mathrm{d}S(Q)$$

and

$$\Delta U_{ij}(Pm, Qn) = \int_{\Delta S_n} U_{ij}(Pm, Q)\, \mathrm{d}S(Q) \tag{16}$$

may be calculated exactly by knowing the size, orientation and location of ΔS_n and the point Pm. The results of these integrals for the case when $Pm = Qn$ are given in Appendix 2. A more complete discussion of all the integrals may be found in [16]. The points Pm and Qn are taken at the centroids of the elements ΔS_n to account best for the variation of u_i and t_i on ΔS_n. Equation (15) may now be written as

$$\sum_n [\{\tfrac{1}{2}\delta_{ij}\delta_{mn} + \Delta T_{ij}(m, n)\}u_j(n)] = \sum_n [\Delta U_{ij}(m, n)t_j(n)], \tag{17}$$

which has the matrix representation

$$\{\tfrac{1}{2}[1] + [\Delta T]\}\{u\} = [\Delta U]\{t\}. \tag{18}$$

The matrix [1] is the identity matrix. In general, the solution to the mixed boundary-value problem is obtained by first appropriately rearranging the columns in equation (18) so that all unknown data appear in the vector $\{x\}$:

$$[A]\{x\} = [B]\{y\}. \tag{19}$$

When rearranging, the columns must be scaled to maintain the proper conditioning of matrix $[A]$. This scaling should maintain the diagonal terms in $[A]$ at the same order of magnitude. Equation (19) has been solved by a standard Gauss reduction scheme on $[A]$ followed by an iteration to refine the solution $\{x\}$. As the matrix $[A]$ is weighted toward the diagonal, it is well conditioned and in actual numerical examples a single iteration usually achieves refinements in $\{x\}$ on the order of $|\{\Delta x/x\}| < 0{\cdot}001$. These examples are discussed in the next section.

Finally, after solving equation (19), the now completely known boundary data may be used to determine the solution for the internal displacements and stresses by direct integration of the identities (9) and (10):

$$u_j(p) = -\sum_n u_i(Qn)\Delta T_{ji}(Qn, p) + \sum_n t_i(Qn)\Delta U_{ji}(Qn, p) \tag{20}$$

and

$$\sigma_{ij}(p) = -\sum_n u_k(Qn)\Delta S_{kij}(Qn, p) + \sum_n t_k(Qn)\Delta D_{kij}(Qn, p). \tag{21}$$

The integrations to determine ΔS and ΔD are presently performed numerically as discussed in [16]. Any number of interior solutions may be made once the boundary solution is obtained. Since the solution is performed at pre-selected points, the analyst may concentrate on particular areas of interest and is not burdened with complete field solutions. No approximations to the field equations are necessary as all approximations are made at the surface.

NUMERICAL RESULTS

1. *Some test problems*

Some elementary boundary value problems were solved to determine the validity of the approximations discussed in the last section as well as to investigate the behavior of the numerical procedures under different circumstances. The computed results are given for a cube with unit dimensions. In all cases sufficient displacements are set to zero to eliminate the rigid body motion. Typical surface element arrangements are shown in Fig. 1 for 12, 24 and 48 surface elements. All results have been obtained using a single, general source program written in Fortran language.† Required data includes the material properties, the surface element arrangement, the known surface tractions and displacements which are assumed constant over each surface element, and the locations of internal points where the displacements and stresses are desired.

In the first series of problems the unit cube is loaded in a state of uniaxial tension by the application of a normal traction to one end. On the other end and on two normal faces the normal displacement component was set equal to zero. The required tractions at these elements are then part of the solution. The surface displacements in the axial and transverse directions are indicated in Fig. 2 for the case of 12 triangles and values of Poisson's ratio varying from one-quarter to one-half. The results for $\nu = 0{\cdot}3$ giving the surface tractions and displacements and internal stresses for twelve and twenty-four surface triangles are

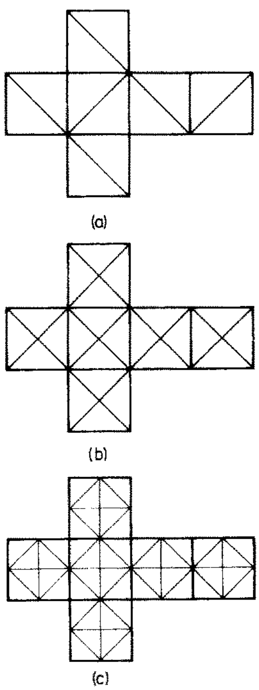

FIG. 1. Surface element arrangements for unit cube.

† All problems in this paper were run on a UNIVAC 1108 computer utilizing external drum storage. A typical run for fifty surface elements and no use of symmetry is around five minutes.

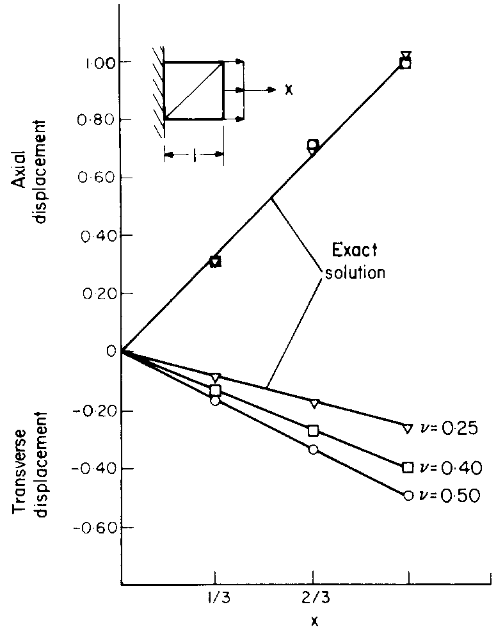

FIG. 2. Surface displacements for the uniaxial model.

given in Table 1. The numerical integrations for the interior stresses are performed to about the same accuracy in both. The second elementary problem was to solve the case for a uniform shear stress applied to the unit cube in one of its planes. This problem was solved for the case of 12, 24 and 48 surface elements. Again sufficient surface displacements were fixed to zero to eliminate the rigid body motion. The results for the non-zero shear strains based on surface displacements and internal stresses at two points are given in Table 2.

A number of features of the method can be seen from these simple examples. First, and most significantly, the basic assumptions of the last section are justified by the very satisfactory results achieved. Also of significant interest is the accuracy with which surface

TABLE 1. PARTIAL DATA FOR THE UNIT CUBE WITH 12 AND 24 ELEMENTS UNDER UNIAXIAL TENSION, p, INCLUDING SURFACE REACTIONS, SURFACE DISPLACEMENTS, AND INTERNAL STRESSES AT THE POINTS (0·4, 0·4, 0·4) AND (0·6, 0·6, 0·6). ONLY TYPICAL RESULTS ARE SHOWN. POISSON'S RATIO = 0·30

		$N = 12$	$N = 24$	Exact
Reactions (t_i/p):		1·000	1·0016	1·0000
		1·000		1·0000
		0·000	0·0006	0·0000
Maximum axial displacement (u_i/δ):		1·025	1·022	1·000
Maximum trans. displacement		1·097	1·032	1·000
Internal stresses:				
	σ_x/p	σ_y/p	τ_{xy}/p	τ_{yz}/p
$N = 12$ (0·4, 0·4, 0·4)	1·030	−0·074	−0·010	0·021
(0·6, 0·6, 0·6)	1·028	−0·077	0·012	−0·034
$N = 24$ (0·4, 0·4, 0·4)	1·031	−0·043	0·004	−0·015
(0·6, 0·6, 0·6)	1·033	−0·044	0·003	−0·014
Exact	1·000	0·00	0·00	0·00

TABLE 2. PARTIAL DATA FOR THE UNIT CUBE LOADED IN PURE SHEAR STRESS, p, IN ONE OF ITS PLANES, INCLUDING COMPUTED SHEAR STRAIN AND SOME INTERNAL STRESSES FOR $N = 12$, 24 AND 48 ELEMENTS. $\gamma_{ref} = p/\mu$.

N	γ_{xz}/γ_{ref}	σ_z/p	τ_{xy}/p	τ_{xz}/p	τ_{yz}/p	
12	0·863	−0·09	−0·02	0·69	−0·002	(0·4, 0·4, 0·4)
		0·06	−0·04	0·67	−0·03	(0·6, 0·6, 0·6)
24	0·957	0·02	−0·05	0·89	−0·05	(0·4, 0·4, 0·4)
		0·02	−0·05	0·89	−0·05	(0·6, 0·6, 0·6)
48	0·960	−0·01	0·02	0·94	0·02	(0·4, 0·4, 0·4)
		−0·009	0·02	0·94	0·02	(0·6, 0·6, 0·6)
Exact	1·000	0·00	0·00	1·00	0·00	

tractions are calculated. This feature is used to full advantage in the example of the fixed-end problem discussed later. It should be noted that refinement of the elements does not affect the displacement results for the uniaxial problem nearly as much as for the shear problem. This is a reasonable result as the shear problem constitutes a greater degree of approximation with the constant displacement assumption on each element. Refinement of the surface elements does lead to improved internal stresses although good results may be achieved for a reasonably small number of surface elements.

2. *The fixed-end problem*

The significant problems of determining three-dimensional stress concentrations are well suited to this analysis procedure. To demonstrate this the three dimensional equivalent to the "Hanging-Plate Problem" was investigated. In this problem a body (again taken as the unit cube as shown in Fig. 3) is loaded by an axial load at one end while the load-

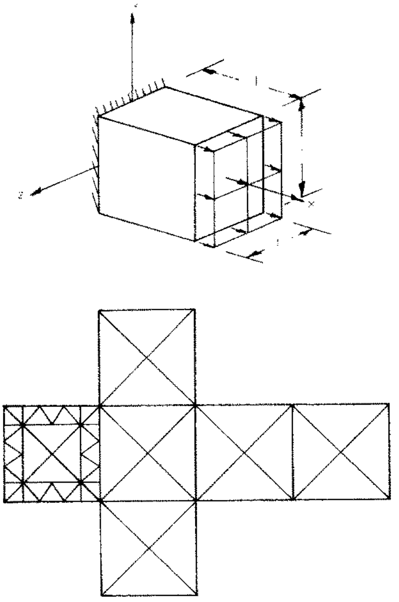

FIG. 3. Surface element arrangements for the fixed end problem.

reacting end is fixed against all motion, including the transverse displacements arising from the non-zero Poisson's ratio. It is known [17] that for the case of plane strain stress singularities of the order $r^{-0.35}$ occur local to the edge. In the three dimensional problem the same behavior is expected at some distance from the corner where plane strain may be said to govern. However, the nature of the singularity at the corner is unknown. It may be expected because of the discontinuous shear stress in both directions at the corner that the stress concentration is going to be greater than that for plane strain. In addition to these two particular behaviors there will be a transition region of, as yet, undetermined extent between the corner solution and the plane strain solution.

As mentioned earlier, the boundary solution of the direct potential method tends to calculate tractions very accurately assuming, of course, a reasonable set of surface elements. Therefore, the cube was divided into surface elements as shown in Fig. 3 with a coarse mesh on all faces except the fixed end. A variety of solutions were obtained for various element arrangements on the fixed end, all based on the one shown. A very important feature of the analysis that was discovered at this time was that a single element at the fixed end could be further subdivided without seriously altering the solution already obtained for the other elements. For example, the results shown in Figs. 5 and 6 were obtained by subdividing one of the corner elements into about twenty elements. The change in the solution at the adjacent elements was less than five per cent. This feature permitted local analysis without the necessity of a prohibitive number of elements on the whole surface.

The results for the normal and shear stresses along a mid-line of the cross-section at the wall are shown in Fig. 4. These results are plotted along with the solution for the circular cylinder obtained by Pickett using Fourier series [18].

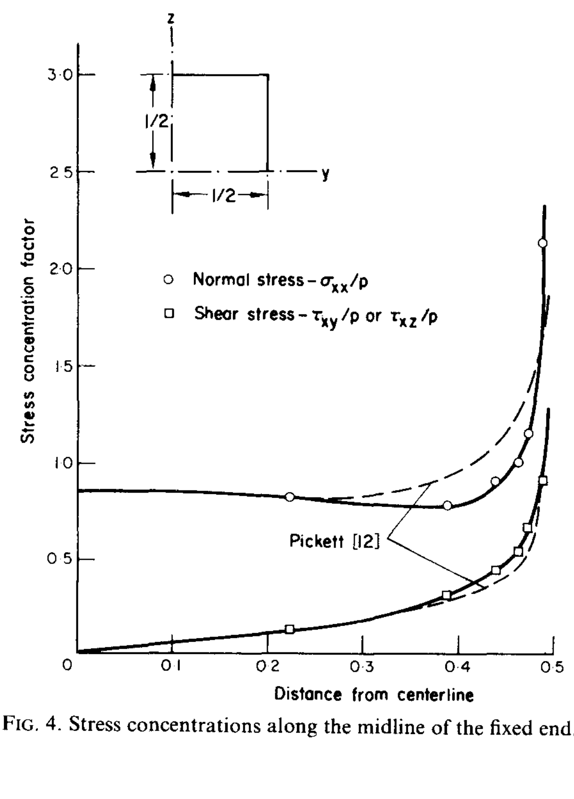

FIG. 4. Stress concentrations along the midline of the fixed end.

The two solutions are essentially the same and the differences between the curves is most likely the effect of the different geometries as Pickett was working with the cylinder. It should also be noted that Pickett complains of the very bad convergence of his series at the end and that as he got near the edge at the fixed end his results no longer converged. No such difficulty is encountered in the direct potential method solution of this problem. The analyst need only refine the surface element sizes to obtain better resolution in areas of high stress gradients.

Of greater interest are the results in the neighborhood of the corner as indicated in Figs. 5 and 6. These figures are machine drawn contour plots of the normal stress concentration and total shear stress $(\tau_{xy}^2+\tau_{xz}^2)^{\frac{1}{2}}$ concentration for the region $\frac{1}{3} \leq y < \frac{1}{2}$ and $\frac{1}{3} \leq z < \frac{1}{2}$. The contours were drawn based on data obtained at more than 30 subelements in the corner. It should be noted that the contours are only drawn to within 0·012 in. of the edge as this was as close to the edge as uniform data was obtained. The stress concentration due to the corner is clearly indicated and, as expected, is considerably greater than that found away from the corner. As indicated in Fig. 5 the normal stress concentration factor even closer to the corner is almost 12. The region of transition from plane strain to the corner condition is also clearly indicated in Figs. 5 and 6. This region appears to be significant to a distance of about ten per cent of the cube width from the edge.

In Fig. 7 the results for the interior stresses σ_x and σ_y are plotted for various lines parallel to the x-axis. The results are extrapolated to the known values at the fixed surface. The

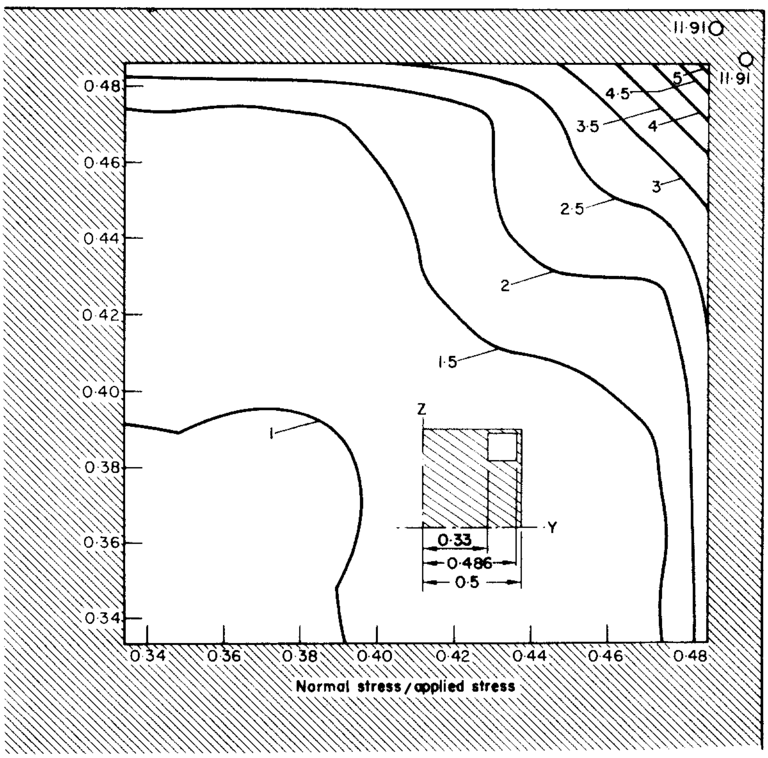

FIG. 5. Normal stress concentrations in the corner.

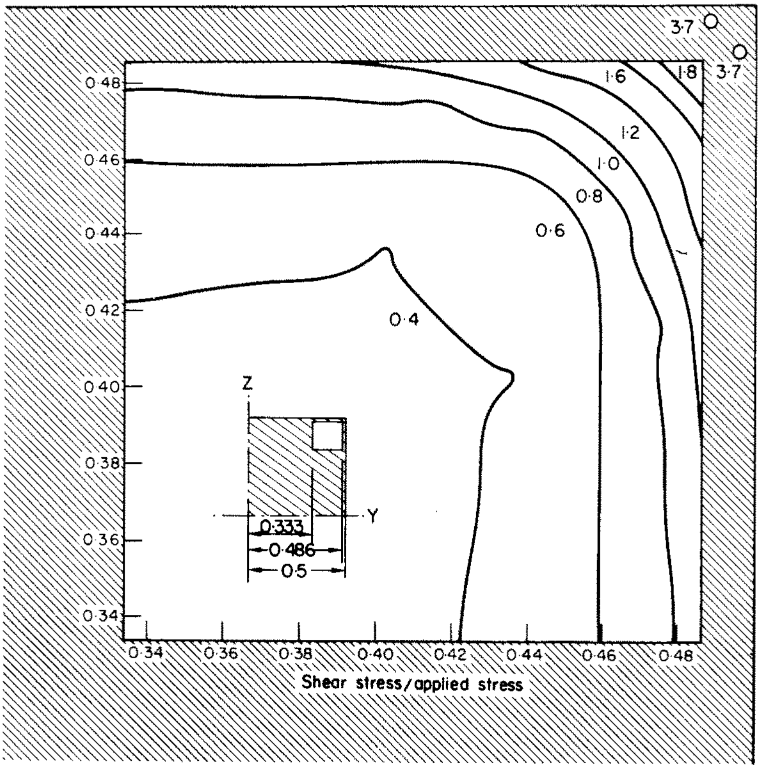

FIG. 6. Total shear stress concentrations in the corner.

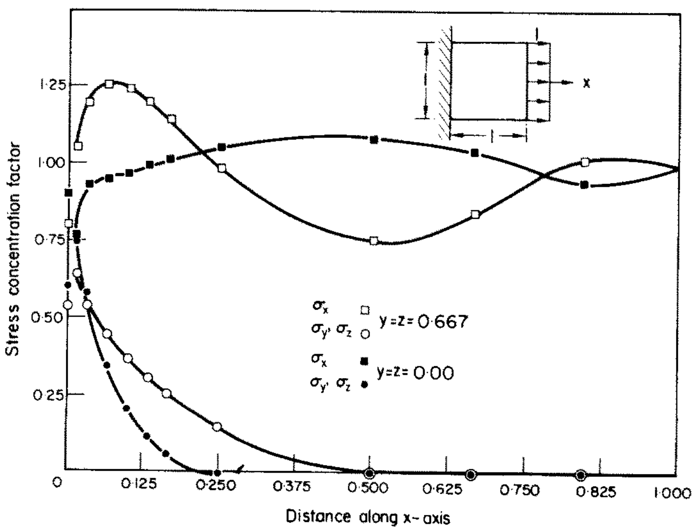

FIG. 7. Internal stresses.

indicated errors for interior points very near the fixed end are attributable to numerically integrating over the r^{-3} singularity in equation (13). This behavior is typical of the method and may be eliminated by numerically calculating the in-plane components at the surface using the surface tractions and surface displacements. A means for doing this is discussed in [4]. Other problems with stress concentrations such as internal cracks and surface notches with various geometries are now being investigated.

Acknowledgements—This present work was supported in part by the NASA Research Grant NGR-39-002-023 and in part under a consulting arrangement with Westinghouse Electric Corporation, Research Laboratories. Thanks are due to J. L. Swedlow and F. J. Rizzo for valuable discussions, to W. Van Buren of Westinghouse for discussions of the exact integrals, and to the Carnegie-Mellon University Computation Center for computer time, and to the referee for valuable comments.

REFERENCES

[1] F. J. RIZZO, An integral equation approach to boundary value problems of classical elastostatics. *Q. appl. Math.* **25**, 83 (1967).
[2] T. A. CRUSE and F. J. RIZZO, A direct formulation and numerical solution of the general transient elastodynamic problem—I. *J. math. Analysis Applic.* **22**, 244 (1968).
[3] T. A. CRUSE, A direct formulation and numerical solution of the general transient elastodynamic problem—II. *J. math. Analysis Applic.* **22**, 341 (1968).
[4] F. J. RIZZO and D. J. SHIPPY, A formulation and solution procedure for the general non-homogeneous elastic inclusion problem. *Int. J. Solids Struct.* **4**, 1161 (1968).
[5] C. K. YOUNGDAHL and E. STERNBERG, Three-dimensional stress concentration around a cylindrical hole in a semi-infinite elastic body. *J. appl. Mech.* **33**, 855 (1966).
[6] J. H. ARGYRIS, Matrix analysis of three-dimensional elastic media, small and large displacements. *AIAA Jnl* **3**, 45 (1965).
[7] D. J. AYRES, A numerical procedure for calculating stress and deformation near a slit in a three-dimensional elastic–plastic solid. NASA Report TM X-52440 (1968).
[8] A. E. H. LOVE, *A Treatise on the Mathematical Theory of Elasticity*. Dover (1944).
[9] N. I. MUSKHELISHVILI, *Some Basic Problems of the Mathematical Theory of Elasticity*, 4th Edition. Noordhoff (1953).
[10] V. D. KUPRADZE, Dynamical problems in elasticity, in *Progress in Solid Mechanics*, Vol. III, edited by I. N. SNEDDON and R. HILL. Wiley (1963).
[11] S. G. MIKHLIN, *Multidimensional Singular Integrals and Integral Equations*. Pergamon Press (1965).
[12] O. D. KELLOGG, *Foundations of Potential Theory*. Dover (1953).
[13] W. VAN BUREN, The indirect potential method for three dimensional boundary value problems of classical elastic equilibrium. Research Report 68-1D7-MEKMA-R2, Westinghouse Research Laboratories, 25 October 1968.
[14] L. H. CHEN and D. G. SCHWEIKERT, Sound radiation from an arbitrary body. *J. acoust. Soc. Am.* **35**, 1626 (1963).
[15] K. M. MITZNER, Numerical solution for transient scattering from a hard surface of arbitrary shape-retarded potential technique. *J. acoust. Soc. Am.* **42**, 391 (1967).
[16] T. A. CRUSE, *The Direct Potential Method in Three-Dimensional Elastostatics*. SM-13, Dept. of Mech. Eng., Carnegie-Mellon University (1968).
[17] M. L. WILLIAMS, Stress singularities resulting from various boundary conditions in angular corners of plates in extension. *J. appl. Mech.* **19**, 526 (1952).
[18] G. PICKETT, Application of the Fourier method to the solution of certain boundary problems in the theory of elasticity. *J. appl. Mech.* **11**, 176 (1944).

APPENDIX 1

Somigliana's identity for the displacement vector at a point $p(x)$ in R is given by equation (9) as

$$u_j(p) = -\int_S u_i(Q)T_{ji}(Q,p)\,dS(Q) + \int_S t_i(Q)U_{ji}(Q,p)\,dS(Q). \tag{1.1}$$

The integrals in equation (1.1) are analogous to double and single layer scalar potentials. These integrals may be rewritten in the form

$$\psi_j(p) = \int_S \sigma_i(Q)T_{ji}(Q, p)\,\mathrm{d}S(Q) \tag{1.2}$$

and

$$\phi_j(p) = \int_S \mu_i(Q)U_{ji}(Q, p)\,\mathrm{d}S(Q). \tag{1.3}$$

Let $P(x)$ be a point on the boundary S of R which is not located at an edge. Equation (1.2) may then be written as

$$\psi_j(p) = \int_S [\sigma_i(Q)-\sigma_i(P)]T_{ji}(Q, p)\,\mathrm{d}S(Q)+\int_S \sigma_i(P)T_{ji}(Q, p)\,\mathrm{d}S(Q). \tag{1.4}$$

If the surface density function $\sigma_i(Q)$ satisfies a Hölder condition on S, it can be shown that the first integral in equation (1.4) is continuous for $p \to P$. If

$$\lim_{p\to P} \psi_j(p) = \psi_j(P)$$

it can be verified that the second integral in equation (1.4) has the discontinuity given by

$$\psi_j(P) = -\int_S [\sigma_i(Q)-\sigma_i(P)]T_{ji}(Q, P)\,\mathrm{d}S(Q)-\tfrac{1}{2}\sigma_j(P)+\int_S \sigma_i(P)T_{ji}(Q, P)\,\mathrm{d}S(Q) \tag{1.5}$$

where the second integral is to be interpreted in the sense of the Cauchy Principal Value. Then

$$\psi_j(P) = -\tfrac{1}{2}\sigma_j(P)+\int_S \sigma_i(Q)T_{ji}(Q, P)\,\mathrm{d}S(Q). \tag{1.6}$$

By similar methods it can be shown that

$$\phi_j(P) = \int_S \mu_i(Q)U_{ji}(Q, P)\,\mathrm{d}S(Q) \tag{1.7}$$

for the density function $\mu_i(Q)$ bounded on the surface. Combining the results of equation (1.6) and equation (1.7) the boundary constraint equation is obtained

$$\tfrac{1}{2}u_j(P)+\int_S u_i(Q)T_{ji}(Q, P)\,\mathrm{d}S(Q) = \int_S t_i(Q)U_{ji}(Q, P)\,\mathrm{d}S(Q). \tag{1.8}$$

Equation (1.8) is strongly suggestive of Fredholm equations for the boundary value problems of the first and second kind. However, the equations are singular due to the presence of the term

$$\frac{1}{r^2}(n_j r_{,i}-n_i r_{,j})$$

in equation (7). That is, it can be shown that

$$\lim_{Q\to P} r^2(P, Q)T_{ij}(P, Q) \neq 0$$

whereas a limit of zero is required for Fredholm kernels. It has been shown [11], however, that the integral equations (1.8) are regular for all admissible values of Poisson's ratio and that the index of the operator $K[u_j]$ in equation (1.8) is zero. Therefore, the Fredholm alternatives apply and all normal problems are soluble.

APPENDIX 2

When the fixed point P and the field point Q are in the same triangles, the kernels U_{ij} and T_{ij} contain singularities of the order $1/r(P, Q)$ and $1/r^2(P, Q)$, respectively. As noted before these integrals are to be evaluated in the sense of the Cauchy Principal Value in that the region very close to the point P is to be excluded from the integral and the integral is to be evaluated as that region shrinks toward zero area. By letting the surface be represented by plane elements it is possible to perform these integrals exactly.

Let the triangle be shown in a local coordinate system with the origin at P such that side 1–2 is parallel to the ζ_1 axis (see Fig. 8). It will be shown that both integrals (16) reduce to path integrals. The results will be obtained only for the path 1–2 as the total result is easily obtained from that.

In the integral of the kernel U_{ij} change to polar coordinates such that the integral (16) becomes

$$\Delta U_{ij} = \lim_{\rho \to 0} \left\{ \frac{1}{4\pi\mu} \int_0^{2\pi} \left[(r(\theta) - \rho) \left(\frac{3-4v}{4(1-v)} \delta_{ij} + \frac{1}{4(1-v)} r_{,i} r_{,j} \right) \right] \mathrm{d}\theta \right\}$$

which, in the limit becomes

$$\Delta U_{ij} = \frac{1}{4\pi\mu} \int_0^{2\pi} r(\theta) \left[\frac{3-4v}{4(1-v)} \delta_{ij} + \frac{1}{4(1-v)} r_{,i} r_{,j} \right] \mathrm{d}\theta.$$

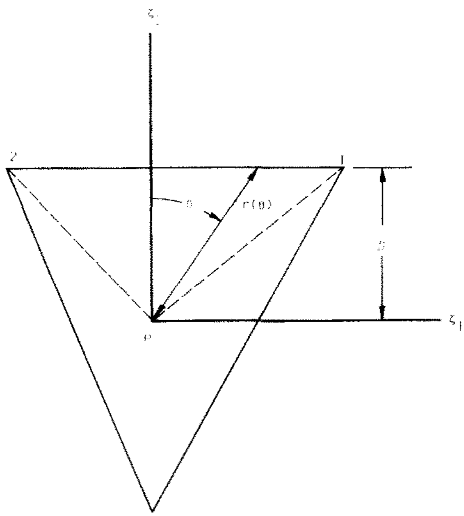

FIG. 8. Scheme for exact integration of ΔU and ΔT.

In the integral of T_{ij} it is seen that, for $\partial r/\partial n = 0$, by using the identity

$$\varepsilon_{ijk}\varepsilon_{rsk}n_r\left(\frac{1}{r}\right)_{,s} = \frac{1}{r^2}(n_j r_{,i} - n_i r_{,j})$$

the integral (16) reduces to

$$\Delta T_{ij} = \frac{k}{4\pi}\varepsilon_{ijk}\int_{\Delta S}\varepsilon_{rsk}n_r\left(\frac{1}{r}\right)_{,s}\,\mathrm{d}s.$$

Using a form of Stokes' theorem this reduces to the line integral

$$\Delta T_{ij} = \frac{k}{4\pi}\varepsilon_{ijk}\oint\frac{1}{r}\,\mathrm{d}x_k.$$

If the variables are now changed to the local variables, then

$$\frac{\partial r}{\partial x_i} = \sin\theta\frac{\partial\zeta_1}{\partial x_i} + \cos\theta\frac{\partial\zeta_2}{\partial x_i} = \sin\theta\, e_{1i} + \cos\theta\, e_{2i}$$

where e_{1i} and e_{2i} are the direction cosines of the ζ_1 and ζ_2 axes in the global coordinate system. Then it is also found that

$$\mathrm{d}x_k = e_{1k}\,\mathrm{d}\zeta_1 + e_{2k}\,\mathrm{d}\zeta_2$$

and along side 1–2 $r(\theta)$ becomes

$$r(\theta) = D/\cos\theta.$$

Finally, by substitution of these results it is found that

$$\Delta U_{ij}|_1^2 = -\frac{D}{4\pi\mu}\left\{\frac{3-4\nu}{4(1-\nu)}\delta_{ij}[\log(\tan\theta + 1/\cos\theta)] + \frac{1}{4(1-\nu)}[e_{1i}e_{1j}(-\sin\theta + \log(\tan\theta + 1/\cos\theta)) + e_{2i}e_{2j}\sin\theta - (e_{1i}e_{2j} + e_{2i}e_{1j})\cos\theta]\right\}\Big|_{\theta_1}^{\theta_2}$$

and that

$$\Delta T_{ij}|_1^2 = \frac{k}{4\pi}\varepsilon_{ijk}e_{1k}[\log(\zeta_1 + r)]|_1^2.$$

The total results are then obtained by reorienting the local coordinate system such that the ζ_1 axis is in turn parallel to the 2–3 and 3–1 sides and adding the contributions. The results are thereby easily obtained in terms of the coordinates of P and the corners 1, 2 and 3 of the triangle.

(*Received* 7 *November* 1968; *revised* 19 *May* 1969)

Абстракт—Дается способность численного решения задач трехмерной статики упругого тела. Метод решения использует сингулярные интегральные чравнения. Можно их решить нумерически, для неизвестных поверхностных усилий и перемещений полной смешаной краевой задачи. Метод не зависит от формы поверхности и подробных данных и вполне автоматиризован. Решаются некоторые простые примеры для проверки формулировки. Кроме этого, используется метод для исследования важной задачи с сингулярностями напряжений.